Paper
Int'l J. of Aeronautical & Space Sci. 17(3), 409–422 (2016)
DOI: http://dx.doi.org/10.5139/IJASS.2016.17.3.409

IJASS
International Journal of Aeronautical and Space Sciences

Parametric Analysis and Design Optimization of a Pyrotechnically Actuated Device

Doo-Hee Han* and Hong-Gye Sung**

Department of Aerospace and Mechanical Engineering, Korea Aerospace University, Gyeonggi 10540, Republic of Korea

Seung-Gyo Jang* and Byung-Tae Ryu******

Advanced Propulsion Technology Center, Agency for Defense Development, Yuseong P.O. Box 35, Daejeon 34060, Republic of Korea

Abstract

A parametric study based on an unsteady mathematical model of a pyrotechnically actuated device was performed for design optimization. The model simulates time histories for the chamber pressure, temperature, mass transfer and pin motion. It is validated through a comparison with experimentally measured pressure and pin displacement. Parametric analyses were conducted to observe the detailed effects of the design parameters using a validated performance analysis code. The detailed effects of the design variables on the performance were evaluated using the one-at-a-time (OAT) method, while the scatter plot method was used to evaluate relative sensitivity. Finally, the design optimization was conducted by employing a genetic algorithm (GA). Six major design parameters for the GA were chosen based on the results of the sensitivity analysis. A fitness function was suggested, which included the following targets: minimum explosive mass for the uniform ignition (small deviation), light casing weight, short operational time, allowable pyrotechnic shock force and finally the designated pin kinetic energy. The propellant mass and cross-sectional area were the first and the second most sensitive parameters, which significantly affected the pin's kinetic energy. Even though the peak chamber pressure decreased, the pin kinetic energy maintained its designated value because the widened pin cross-sectional area induced enough force at low pressure.

Key words: Pyrotechnically actuated device, Performance analysis, Sensitivity analysis, Genetic algorithm optimization

1. Introduction

Pyrotechnically actuated devices (PAD) are actuated by highly metalized charges such as ZPP or BKNO3. They have high energy densities and fast reactivity so as to enable a robust actuation with a small chamber volume. A PAD can be adopted for various purposes by simply changing the working mechanism of the movable piston [1]. Typical PAD types are pin puller, explosive bolt, line cutter, pyro valve [2]. Due to the crucial positioning and function of a PAD, a misfire could lead to the destructive failure of an entire mission. Small changes in design parameters could seriously affect the device's performance because a PAD uses a small amount of highly reactive charges in a small device. Moreover, relatively large deviations could occur during the manufacturing process. Thus, understanding the effects of parameter changes on performance is vital to avoid unexpected malfunctions. The pin puller device is mainly discussed in this paper.

The pin puller device is designed to detach two objects simultaneously. The pin puller has a main driving pin as well as explosion and expansion chambers connected by a port. The pin puller also includes another driving pin that protrudes outward to bind the device to an object that is inserted into the expansion chamber. Small granule type pyrotechnic initiators such as ZPP and BKNO3 are then loaded inside the explosion chamber so that hot gases are rapidly generated when ignited.

* Ph. D Student
** Professor, Corresponding author: hgsung@kau.ac.kr
*** Principal Researcher: jsg4580@add.re.kr
**** Principal Researcher: btryu@add.re.kr

Received: November 9, 2015 Revised: August 22, 2016 Accepted: September 14, 2016

http://ijass.org pISSN: 2093-274x eISSN: 2093-2480

The hot gas flows into the expansion chamber through a port and pushes the driving pin via its high pressure. When the pressure force exceeds the ultimate strength force of the shear pin, the main pin is continuously driven by the high pressure gas. When the protruding portion of the driving pin shrinks into the device, the pin puller is able to detach an object instantaneously. Compared to electrically driven devices such as servo actuators, a PAD cannot be reused and is hard to control once it has been activated. However, the PAD only requires a small current to ignite the charges, which results in smaller battery requirements and greater reliability. Also the high internal pressure makes the device carries out the mission robustly and instantaneously. Its characteristics (greater power, instant reactivity, light weight and reliability) make it suitable for various aerospace and defense applications.

PAD have simple working mechanisms, but precise design is difficult because the design parameters are coupled to one another [3]. Due to the complex phenomena and high reliability requirements, PAD development has thus far relied on repeated experiments to achieve appropriate designs. Recently however, several researchers have been able to successfully carry out mathematical modeling to predict PAD performance. Gonthier et al. [4] suggested a zero-dimensional, quasi-steady state mathematical model for a pin puller. Paul et al. [5] formulated a quasi-one-dimensional model to account for the unsteady gas dynamic effect in the pyrotechnic valve. They also conducted a parametric study and revealed that the cross-sectional area of the connecting port controlled the energy transport rate. Lee [6] revealed that the unsteady gas dynamic effect could not be negligible when the operation time was in the range of the characteristic gas dynamics timescale of the device. Also, Lee [7] suggested the importance of a heat loss model. He addressed how heat loss significantly affected the device's performance even when it only worked for a short period of time. Powers et al. [8] performed a sensitivity analysis by simply changing the parameter value. They analyzed the sensitivity of a radiative and convective heat transfer coefficient and burning rate. They also found a limitation in parameter variations that affected the device's performance.

The objective of this paper is to understand the fundamental functions and sensitivity of the design parameters of a PAD and to find a design optimization point. The entire process was performed through a sequential work-flow of performance analysis, sensitivity analysis and genetic algorithm (GA). Before the optimization process was carried out, a proposed mathematical performance analysis model was established and validated. The unsteady state model considering continuity, heat balance and solid phase effects are fabricated with conservation equations. A thermodynamic properties library was constructed using NASA's Chemical Equilibrium with Applications (CEA) code. Next, two sensitivity analyses were conducted to evaluate the influence of the design parameters on the pin puller's performance. First, the one-at-a-time (OAT) method [9] was employed to observe how the detailed parameter deviation affected performance. Second, the scatter plot method was used to investigate the relative sensitivity [10]. Combining the results of these two methods provided an understanding of the role and importance of each design parameter. After the sensitivity analyses, the key design parameters were selectively chosen so as to establish the fitness function for the GA optimization. Finally, the multi-objective GA optimization (designed to balance performance and device weight) was conducted. In this study, the term performance refers to the desired pin kinetic energy, the minimum charge mass for uniform ignition, a short operational time and the minimum required pyrotechnic shock force.

2. Mathematical model

Figure 1 shows the schematics of the pin puller. It was largely separated into two sections for greater modeling simplicity. First, the explosion chamber was reserved for ZPP granule combustion. During ZPP combustion, this section experienced the mixing effects of the air and gas, the mass flow rate of the gas moving out through the port and the pressure and temperature change rates in the explosion chamber. The other section was an expansion chamber. It experienced gas mixing, pressure and temperature change rates and pin movement. The two sections were simultaneously coupled by mass and energy flows through the port. Here, the mass flow is the sum of the gas and the condensed phase where the distribution ratio is assumed to be the same as the ratio in the chamber. The heat transfer rate between the gas and the condensed phase was assumed to be infinitely fast so that the temperature of both phases was considered to be equal.

The explosion chamber contained ZPP granules consisting of zirconium. It thus generated both gas and condensed phase products [11]. As with typical metal based explosive devices, the condensed combustion product occupied most of the volume so that multi-phase modeling had to be performed. The solid ZPP charges and condensed phase combustion products were incompressible, while the compressible gas phase products were modeled under the perfect gas law assumption.

The combustion of solid ZPP was simulated according to

Saint Robert's law, which models a burn rate as a function of pressure. The entire model assumed that the combustion process was in a state of equilibrium at each time step (quasi-steady state). Therefore, the ZPP combustion results, including the thermodynamic properties of the combustion products, condensed phase ratio and heat release per unit volume were all calculated using the CEA [12] code. The CEA results were extracted as a function of pressure (1~4000 bar, every 1 bar) and written as a library to reduce the computational time necessary for repeated calculations such as those required for the sensitivity analysis and GA optimization. Table 1 shows the reaction formula used when constructing the ZPP combustion library.

Table 1 shows that the ratio of combustion products change along the chamber pressure. The Viton, used as a binder, was ignored as it takes up only a small portion of the ZPP formula. The last term, $ZrO_2(L)$, denotes Zirconium dioxide in its liquid phase, which did not provide any contribution to the pressure build-up process. The void volume caused by the solid charge and condensed phase was taken into account to more accurately predict the pressure. The pressure slope was derived using an ideal gas equation of state and mass conservation while temperature slope was derived from the energy balance equation. Air was used as the initial gas composition of the chamber and then a blend of combustion gas was simulated using the mass weighted mixing law.

The volume expansion in the expansion chamber resulting from the piston displacement was accounted for. In a pin puller device, combustion gas flows through the port and causes the pressure to increase in the expansion chamber. This continues until the point at which the shear pin ruptures. This means that the effects of volume expansion and the work done by the expansion should be included in the pressure and temperature model equations. The pressure force on the driving pin can be calculated easily, but the friction force coefficient needs to be obtained experimentally. If the total forces on the pin are accurately calculated, the position, velocity and acceleration of the pin can be obtained using Newton's second law.

The governing equations based on mass and momentum conservation at the explosion chamber are

$$\dot{m}_1 = \dot{m}_{gen} - \dot{m}_{port} \tag{1}$$

$$\frac{d(E_{sys.1})}{dt} = \dot{E}_{in.1} - \dot{E}_{out.1} \tag{2}$$

$$P_1 V_1 = m_{g1} R_1 T_1 \tag{3}$$

where the energy balance terms are expressed as

$$\frac{d(E_{sys.1})}{dt} = \frac{d(m_{g1} c_{v.g1} T_1)}{dt} + \frac{d(m_{cp1} c_{v.cp1} T_1)}{dt} \tag{4}$$

$$\dot{E}_{in.1} = (1-\eta_{cp})\left(\dot{m}_{gen} c_{p.g.gen} T_{gen}\right) + (\eta_{cp})\left(\dot{m}_{gen} c_{p.cp.gen} T_{gen}\right) \tag{5}$$

$$\dot{E}_{out.1} = (1-\eta_{cp})\left(\dot{m}_{port} c_{p.g1} T_1\right) + (\eta_{cpt})\left(\dot{m}_{port} c_{p.cp1} T_1\right) + \dot{Q}_{loss.1} + \dot{W}_{work} \tag{6}$$

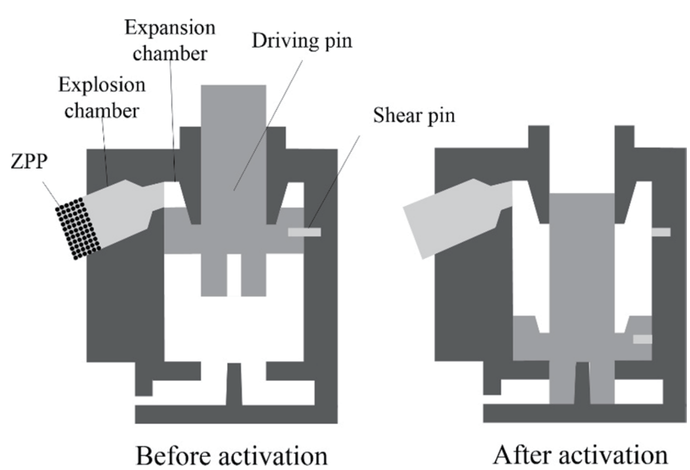

Fig. 1. Pin puller schematics

Table 1. ZPP combustion reaction formula (reference case)

$$\begin{aligned} 4.0908\mathrm{Zr} + 2.9178\mathrm{KCLO_4} \\ &= a\mathrm{CL(g)} + \mathrm{bCLO(g)} + \mathrm{c}CL_2\mathrm{(g)} + \mathrm{dK(g)} + \mathrm{eKCL(g)} \\ &+ \mathrm{fKO(g)} + \mathrm{g}K_2\mathrm{(g)} + \mathrm{h}K_2CL_2\mathrm{(g)} + \mathrm{iO(g)} + \mathrm{j}O_2\mathrm{(g)} \\ &+ \mathrm{k}O_3\mathrm{(g)} + \mathrm{lZrO(g)} + \mathrm{m}ZrO_2\mathrm{(g)} + \mathrm{n}ZrO_2\mathrm{(L)} \end{aligned}$$

In the above equations, subscripts 1 and 2 are used to label the explosion and expansion chamber quantities, respectively. Subscripts g and *cp* represent the gas phase and condensed phase quantities, respectively. η_{cp} is a mass fraction of the condensed phase of the combustion products as represented as $\eta_{cp}=m_{cp}/(m_{cp}+m_{cp})$. Also c_p and c_v are the constant pressure and constant volume of specific heat, respectively. T_{gen} is the adiabatic flame temperature of the propellant. All of the variables above are calculated using the CEA code at every time step. $\dot{m}_{gen}$ is the total mass generation rate from the propellant, which can be calculated using

$$\dot{m}_{gen} = \rho_p A_b r_b \tag{7}$$

Variables ρ_p, A_b and r_b represent the solid propellant density, burning area and burning rate, respectively. The burning rate (r_b) is a function of the chamber pressure. It follows Saint Robert's law,

$$r_b = aP^n \tag{8}$$

Also, the total burning area of the propellants ( ) can be expressed as a function of the granules number (N) and the surface area of a granule.

$$A_b = N \cdot 4\pi (D/2)^2 \tag{9}$$

The mass flow rate of the gas flowing through the port ($\dot{m}_{port.g}$) is formulated using conventional gas dynamics equations [13].

$$\dot{m}_{port.g} = \begin{cases} \rho_{g1} A_e \sqrt{\dfrac{2\gamma_1 R_1 T_1}{\gamma_1 - 1}\left(\dfrac{P_1}{P_2}\right)^{-\frac{\gamma_1+1}{\gamma_1}}\left(\left(\dfrac{P_1}{P_2}\right)^{\frac{\gamma_1-1}{\gamma_1}} - 1\right)} & \textbf{if } \left(\dfrac{P_1}{P_2}\right) < \left(\dfrac{\gamma_1+1}{2}\right)^{\frac{\gamma_1}{\gamma_1-1}} \quad (Non-Chocked) \\ \rho_{g1} A_e \sqrt{\gamma_1 R_1 T_1}\left(\dfrac{2}{\gamma_1+1}\right)^{\frac{\gamma_1+1}{2(\gamma_1-1)}} & \textbf{if } \left(\dfrac{P_1}{P_2}\right) \geq \left(\dfrac{\gamma_1+1}{2}\right)^{\frac{\gamma_1}{\gamma_1-1}} \quad (Chocked) \end{cases} \tag{10}$$

The mass flow rate of the condensed phase through the port is assumed to have the same composition ratio as the gas and condensed phase in the explosion chamber. It is expressed as

$$\dot{m}_{port.cp} = \left(\frac{n_{cp}}{1-n_{cp}}\right)\dot{m}_{port.gas} \tag{11}$$

With these equations, the pressure and temperature change-slopes are obtained.

$$\frac{dP_1}{dt} = \frac{\dot{m}_{g1}R_1T_1 + M_{g1}R_1\dot{T}_1 - P_1\dot{V}_1}{V_1} \tag{12}$$

$$\frac{dT_1}{dt} = \frac{\left(\dot{E}_{in.1} - \dot{E}_{out.1} - (1-\eta_{cp})\dot{m}_1 c_{v.g1} T_1 - \eta_{cp}\dot{m}_1 c_{v.cp1} T_1\right)}{(1-\eta_{cp})M_1 c_{v.g1} + \eta_{cp} M_1 c_{v.cp1}} \tag{13}$$

Here the volume change rate in the explosion chamber, $\dot{V}_1$, considers the effects of a void volume resulting from the burning of the granules as well as the effects of a volume occupied by the condensed combustion products.

$$\dot{V}_1 = A_b r_b - \rho_s (A_b r_b \eta_{cp}) / \rho_{cp} \tag{14}$$

$Q_{loss.1}$ in Equation (7) is the heat loss resulting from convection and radiation from a surface of the device into the surroundings.

$$Q_{loss.1} = hA_{w.1}(T_{w.1} - T) + \sigma A_{w.1}\left(T_{w.1}^4 - T^4\right) \tag{15}$$

In the same manner, the conservation equations for the expansion chamber can be expressed as per Equations (17) through (19). The total mass flow rate and energy transfer rate through the port is equivalent to the inlet mass flow rate and energy transfer rate at the expansion chamber.

$$m_2 = m_{port.g} + m_{port.cp} \tag{16}$$

$$\frac{d(E_{sys.2})}{dt} = \dot{E}_{out.1} \tag{17}$$

$$P_2 V_2 = M_{g2} R_2 T_2 \tag{18}$$

As a result, the pressure and temperature slopes for the expansion chamber can be expressed as

$$\frac{dP_2}{dt} = \frac{\dot{m}_{g2}R_2T + M_{g2}R_2\dot{T}_2 - P_2\dot{V}_2}{V_2} \tag{19}$$

$$\frac{dT_2}{dt} = \frac{\left(\dot{E}_{out.1} - (1-\eta_{cp})\dot{m}_2 c_{v.g2} T_2 - \eta_{cp}\dot{m}_2 c_{v.cp2} T_2 - \dot{W}\right)}{(1-\eta_{cp})M_2 c_{v.g2} + \eta_{cp} M_2 c_{v.cp2}} \tag{20}$$

In Equation (21), $\dot{W}$ is the work completed by the pin movement. This term represents one of the reasons that the temperature rapidly decreases after combustion takes place. The volumes of the explosion and expansion chambers (V_1

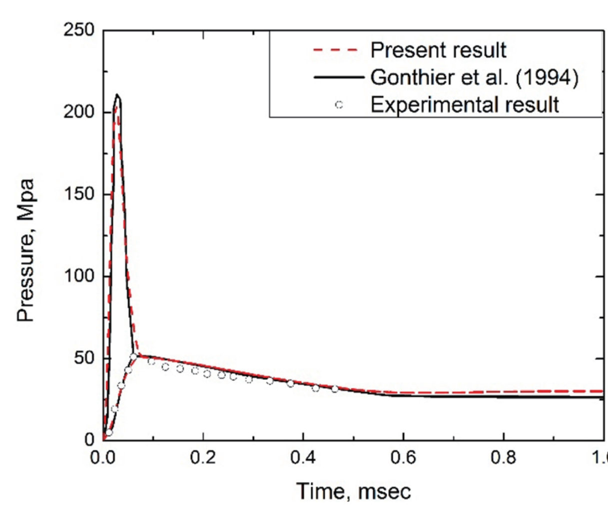

Fig. 2. Chamber pressure validation with a NASA NSI driven pin puller [14]

and V_2) are initially fixed. They then gradually increase as the ZPP is consumed and the pin shaft moves. This leads to a change in the chamber pressure (P). Thus, the volume change rates are calculated with the equations below.

$$\dot{V}_1 = A_b r_b \tag{21}$$

$$\dot{V}_2 = A_p v_p \tag{22}$$

Equation (22) denotes the void volume changing rates of an explosion chamber resulting from ZPP combustion, while Equation (23) denotes the expansion chamber volume expansion rate. The pin velocity can be calculated with a differential form of pin acceleration.

$$\frac{dv_p}{dt} = \frac{F}{M_p} = \frac{F_p - F_f}{M_p} \tag{23}$$

F_p and F_f denote the pressure and friction forces, respectively, acting on the pin. M_p is the mass of the driving pin. Each force is calculated using the following equations.

$$F_p = A_p P_2 \tag{24}$$

$$F_f = 0.03436 + \{191.8 + 0.0102 \times (P_c \times 0.000145)\} \tag{25}$$

$$F_{pf} = F_p - F_f \tag{26}$$

Equation (25) assumes the pressure over the pin cross section is uniformly distributed so that multiples of the pin area and expansion chamber pressure become the pressure force on the pin. Finally, the pyrotechnic shock force, F_{pf}, is the force required to hold the device during its activation.

3. Validation

Before conducting the GA optimization, it is essential to validate the performance analysis code based on the mathematical model listed in section II. The calculated chamber pressure and pin displacement were compared with the experimental data from a NASA NSI driven pin puller and the model simulation data from the work conducted by Gonthier et al [14].

Figure 3 depicts a pressure comparison with the experimental data from a NASA NSI driven pin puller. A split in the lines occurs early on. The upper curve at the initial phase represents the pressure of the explosion chamber, while the lower curve is that of the expansion chamber. The black solid line is the predicted data from Gonthier et al. [14], while the white dots are the experimentally obtained pressure data from the expansion chamber. The results of this paper fit well with the previous study. The calculated pressure at the end of the sequence, however, is slightly lower than that of Gonthier's because of the different thermodynamic properties, including the condensed phase and specific heat ratio. Fig. 3 displays the predicted pin displacement of the current and previous study. The current prediction is faster than Gonthier's even though the same pin friction coefficient was used. This occurred because the pressure in the current study was predicted to be higher than in the previous study. However, the validation test showed an acceptable level of accuracy, so the current research proceeded along the liens of the model suggested above.

4. Performance analysis

A performance analysis was conducted to observe detailed phenomena during the activation of the device. The reference experiment was operated by the Agency for Defense Development in Korea. This equipment used a pin puller device using ZPP as an explosive charge. ZPP masses of 33.4 and 42.9 mg were loaded and tested. Detailed parameters are listed in Table 2.

Both the expansion chamber pressure and pin displacement were measured during the 33.4- and 42.9-mg ZPP mass experiments. The applied mathematical model adequately suited the experiments employed for this study, as shown in Fig, 4. The peak pressure was well predicted in all cases. The decrease in pressure after the peak point was caused by volume expansion. However, an error emerged in the pressure descending sequence with the increase in the amount of ZPP. The primary cause of this error was most likely the infinitely fast heat transfer rate between the two phases [16]. The model treats gas and condensed phase temperatures as being equal even though differences may

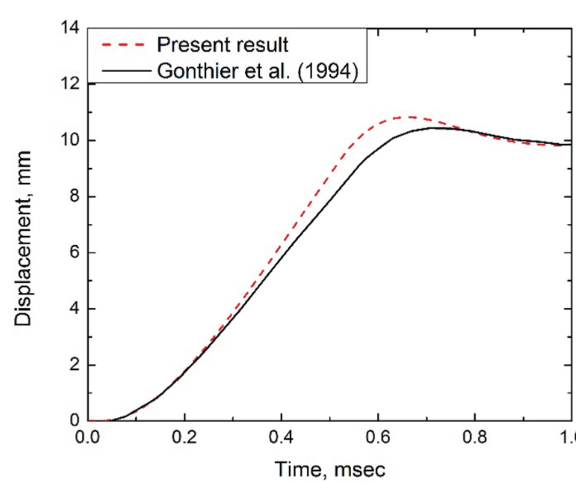

Fig. 3. Pin displacement validation with a NASA NSI driven pin puller [14]

have existed over time. In normal, real world conditions, when the pin moves, the gas temperature should decrease faster than that of the condensed phase because the effects of volume expansion are derived from the energy of the gas phase rather than the condensed phase. However, the model uses the enthalpies of the gas and condensed phase equally during expansion. Since the stored energy in the condensed phase is useless, the model overestimates the useful energy inside the chamber. Thus, the driving pin moves faster with high energy (pressure) and this results in a more rapid decrease in the pressure curves.

Figure 5 depicts the pin kinetic energy of two different ZPP loading amounts. The pin kinetic energy reached its maximum at the end of the stroke. Because the model ignores elastic and damping forces produced at the pin collision, the kinetic energy suddenly dropped to zero at a stopper located at the maximum stroke of the pin. The maximum pin kinetic energy is a crucial factor as it defines the performance of the device or design constraints. Fig. 6 displays the pyrotechnic shock forces during the device's operation. The pyrotechnic shock, which is defined as the required force for the device to hold during activation, showed a similar tendency to that of the pressure curves. Thus, the maximum pyrotechnic shock forces did not occur at the maximum kinetic energy, but rather at the maximum pressure.

Table 2. Design parameters of the validation model [15]

Parameter	Value
Burning rate exponent	0.182
Burning rate constant	0.741 (inch/sec)
Solid density	2.44 (g/cm^3)
Diameters of ZPP	48 (μm)
Explosion chamber volume	0.212 (cm^3)
Initial pin position	2.02909 (cm)
Pin area	2.2966 (cm)
Cap collision point	0.77 (cm)
Shear pin ultimate strength	123 (N)
Port area	0.1256 (cm^2)

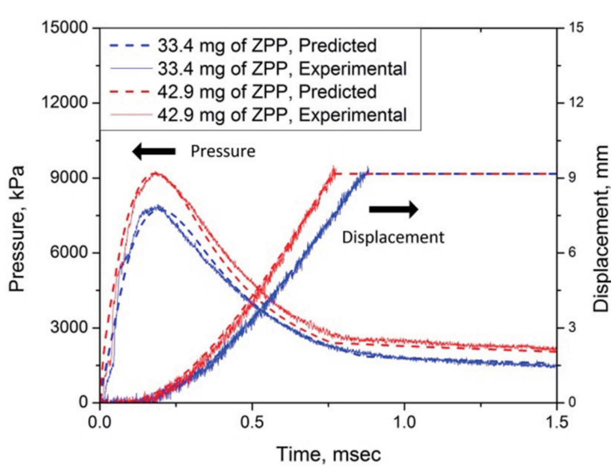

Fig. 4. Predicted and measured expansion chamber pressure histories at different ZPP masses

5. Performance optimization

5.1 Sensitivity analysis for the determination of major design variables

Prior to the GA optimization, it is also necessary to select

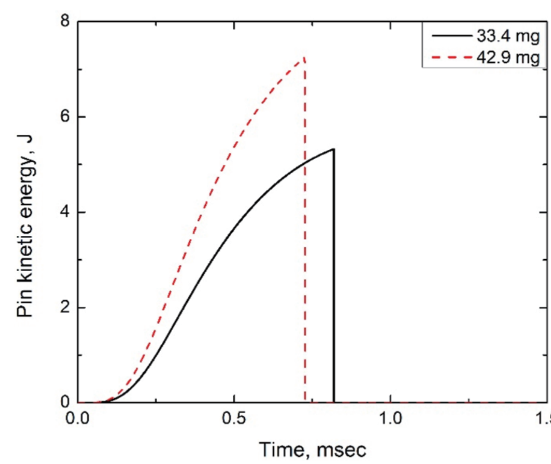

Fig. 5. Pin kinetic energy

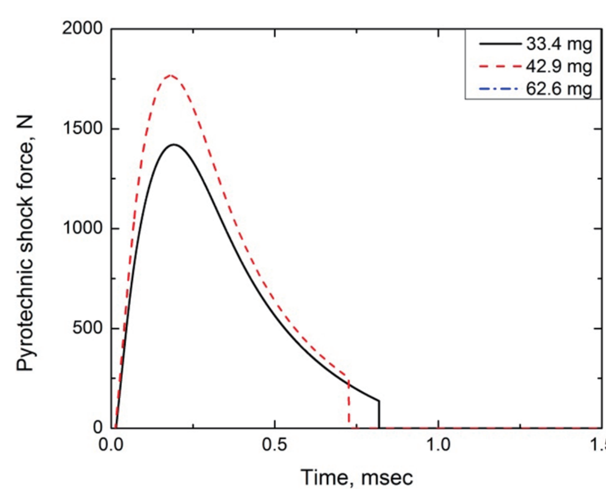

Fig. 6. Pyrotechnic shock forces

DOI: http://dx.doi.org/10.5139/IJASS.2016.17.3.409

the key design parameters. This is because the GA analysis, including all of the variables, would otherwise not be appropriate in terms of efficiency and accuracy. Selecting the variables sensitive to performance is a difficult task since most of the variables are intricately coupled. One of the solutions chosen in this work is a sensitivity analysis. It was conducted using two methods. First, the one variable at a time (OAT) method was employed to see the detailed effects on the entire output when only one variable was changed. Second, the scatter plot method enabled an evaluation of the relative sensitivity.

The OAT analysis was conducted for eight parameters – the explosion chamber volume, pin cross-sectional area, pin mass, initial pin position, total pin stroke, ZPP diameter, loaded ZPP mass and connecting port area. The variables changed in the range of 50 to 150 % of the reference values at 10 uniformly distributed intervals. The unique effects of each parameter on the pin puller pressure curve are shown in Fig. 7. The mass variation of the ZPP had the most dramatic effect on peak pressure, as shown in the Figure 7 (a). It decreased to 5,000 Kpa when 50% of the reference mass was loaded. On the other hand, it increased up to 12,000 Kpa when the ZPP mass was 150% overloaded. The increased ZPP mass induced high pressures and temperatures due to its internal enthalpy and the mass of the gas. Interestingly, the amount of time that expired from zero to peak pressure hardly changed even though the masses were increased. Fig. 7 (b) shows the second sensitive parameter, the pin cross-sectional area.

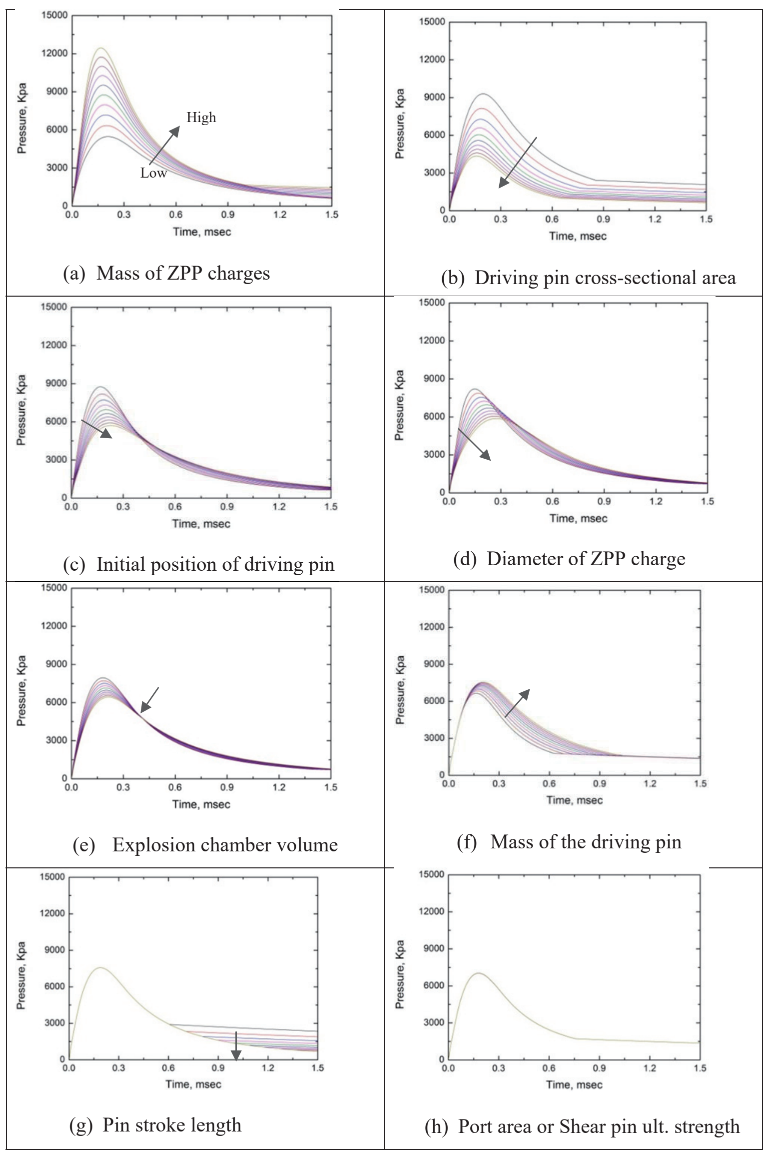

Fig. 7. One at a time (OAT) sensitivity analysis for individual parameter study

The pin area directly affects the volume of the expansion chamber so that an increased pin area results in a lower peak pressure. Here, note that the pressure curves do not cross each other, while in some other cases, such as with the initial pin position, ZPP diameter or chamber volume, the curves crossed during activation. Crossed curves occurred because the large chamber pressure pushed the pin with greater power and this caused faster pin velocities. The higher rate of volume expansion accelerated the rate at which the pressure decreased. When the cross-sectional pin area was enlarged, however, the pressure force acting on the pin did not change as much. This was because the large pin area compensated for the lower chamber pressure. The initial position of the driving pin and the ZPP diameter had similar tendencies. Lowered values induced the chamber pressure to increase and vice versa. The time to peak pressure point was notably different. From Fig. 7 (c), it is evident that the variation in the initial pin position slightly affected the time required to reach peak pressure since a decreased chamber volume induced a faster pressure build-up time and the high pressure induced a faster burning time. However, as depicted in Fig. 7 (d), the decreased ZPP diameter had a stronger effect since it directly widened the effective ZPP granule area. The diameter was the strongest parameter in terms of changing the time to peak pressure. A shrunken explosion chamber volume resulted in a higher peak chamber pressure as the entire volume decreased, as described in Fig. 7 (e). The increased pressure caused the pin velocity to increase in speed so that the pressure curves crossed each other in the decreasing region. Despite this, there were no dramatic differences in the overall performance. From Fig. 7 (f), it can be seen that the mass of the driving pin had no influence on the chamber pressure until the shear pin ruptured. Due to the higher inertia of a heavier pin, the pressure continued to increase even after the shear pin ruptured and vice versa. The pressure curves at different pin stroke lengths did not change before the pin reached the end wall. The final steady state chamber pressure differed because the stroke was related to the total chamber volume. Finally, unlike the results in Paul et al. [5], Figs. 7 (g) and (h) show that the connecting port area and ultimate strength of the shear pin barley affected the performance in this variance range because the overall pressure at the explosion chamber was far lower (maximum peak pressure of 12 MPa) than that of Paul's device (maximum peak pressure of 450 MPa).

The OAT method is an adequate means of determining an individual parameter's detailed effects on overall performance. However, this method cannot evaluate relative sensitivity, especially in a complex problem like that of the pin puller. Relative sensitivity offers more practical, more accurate data for the selection of a design parameter. This can be achieved via the scatter plot method, which is conducted by multiplying the independent random numbers to all performance-affecting pin puller variables. Reasonable data can be acquired by repeating the calculation 10,000 times. In this way, the relative sensitivity on pin puller performance was evaluated for each variable. Fig. 8 shows the results of the sensitivity analysis in the form of a scatter plot. The y axis in the graphs is set to the chamber pressure and pin kinetic energy, while the x axis is assigned to the variance of each individual parameter. Both the expansion chamber pressure and the pin kinetic energy were chosen as output performances since the efficiency of a pin puller is decided by the moving behavior of the pin, while the pressure governs the overall performance.

A total of nine parameters – the ZPP mass, pin area, initial pin position, explosion chamber volume, ZPP diameter, pin stroke, pin mass, ultimate shear pin strength and port diameter – were tested to evaluate their sensitivity on the maximum chamber pressure and pin kinetic energy. In the scatter plots, the shape of a particle clouds moves closer to the linear line when the variable is sensitive relative to the other variables. In Fig. 8, the parameters are lined up in order of pressure sensitivity. Different relative sensitivities definitely exist from the ZPP mass to the explosion chamber volume. A positive sloped centerline, like that in Fig. 8 (a), denotes that the parameter variation is proportional to output. The tendencies of the pressure and pin kinetic energy is similar to most variables, except for the pin cross-sectional area (Figs. 8 (c) and (d)). This is because a higher chamber pressure pushes the pin with stronger force. Essentially, a wide pin cross-sectional area induces a low maximum chamber pressure due to an increased expansion chamber volume. However, the wide pin area accepts higher pressure forces even though the overall pressure decreases. This allows the pin kinetic energy to increase in a low pressure environment. Since the use of shapes to compare the relative sensitivity of each parameter does not provide sufficient clarity, a method of quantifying the values is adopted to evaluate the sensitivity more precisely.

Expressing shapes via a scalar number is a statistical method of comparing the relative sensitivity of all parameters. Fig. 9 represents the quantitative sensitivity schematics using the average distance of individual points to the statistical centerline. The average shortest distance of the points to the centerline, lavg, can be evaluated using

$$l_{avg} = \frac{1}{n}\sum_{i=1}^{n} l_i \tag{27}$$

where n is the number of samples and li is the shortest length from the particle to the centerline. This is similar in meaning to standard deviation, σ. A sharp shape cloud should have a small distance number, while a circle-like cloud should have a large distance number. Table 3 shows the normalized average distance of the cloud in a scatter plot. The distance of each parameter has been normalized by the distance of the most insensitive parameter. It shows the ZPP mass as being the most sensitive factor for both maximum pressure and pin kinetic energy, while the port area is the most insensitive factor. However, the sensitivity order for pressure is different from that of the pin kinetic energy. The pin stroke is more sensitive to the maximum pin kinetic energy than it is to the maximum chamber pressure. The ZPP diameter is more insensitive to the maximum pin kinetic energy than it is to the maximum chamber pressure. Interestingly, the table shows the mass of the pin as being insensitive not only to the maximum pressure but also to the maximum pin kinetic energy. This is because the pin velocity, which is more

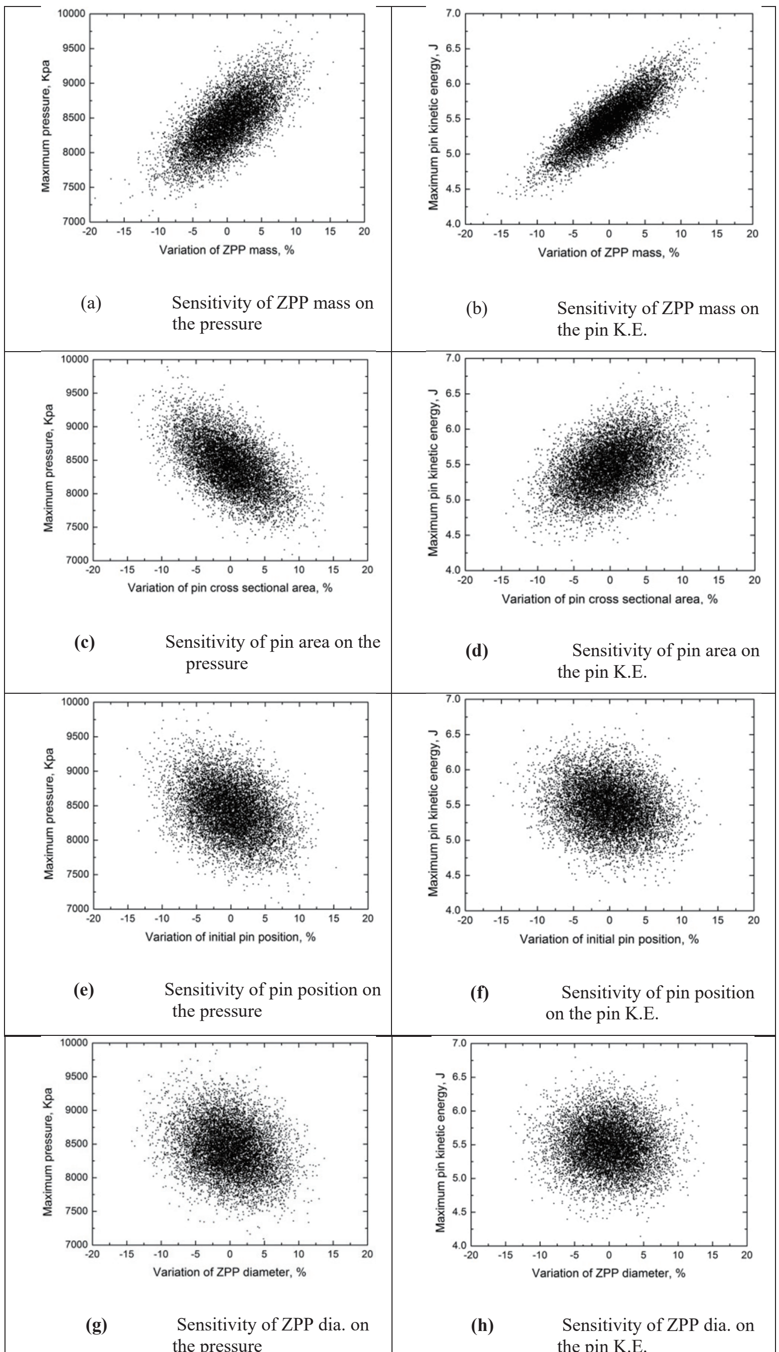

(a) Sensitivity of ZPP mass on the pressure

(b) Sensitivity of ZPP mass on the pin K.E.

(c) Sensitivity of pin area on the pressure

(d) Sensitivity of pin area on the pin K.E.

(e) Sensitivity of pin position on the pressure

(f) Sensitivity of pin position on the pin K.E.

(g) Sensitivity of ZPP dia. on the pressure

(h) Sensitivity of ZPP dia. on the pin K.E.

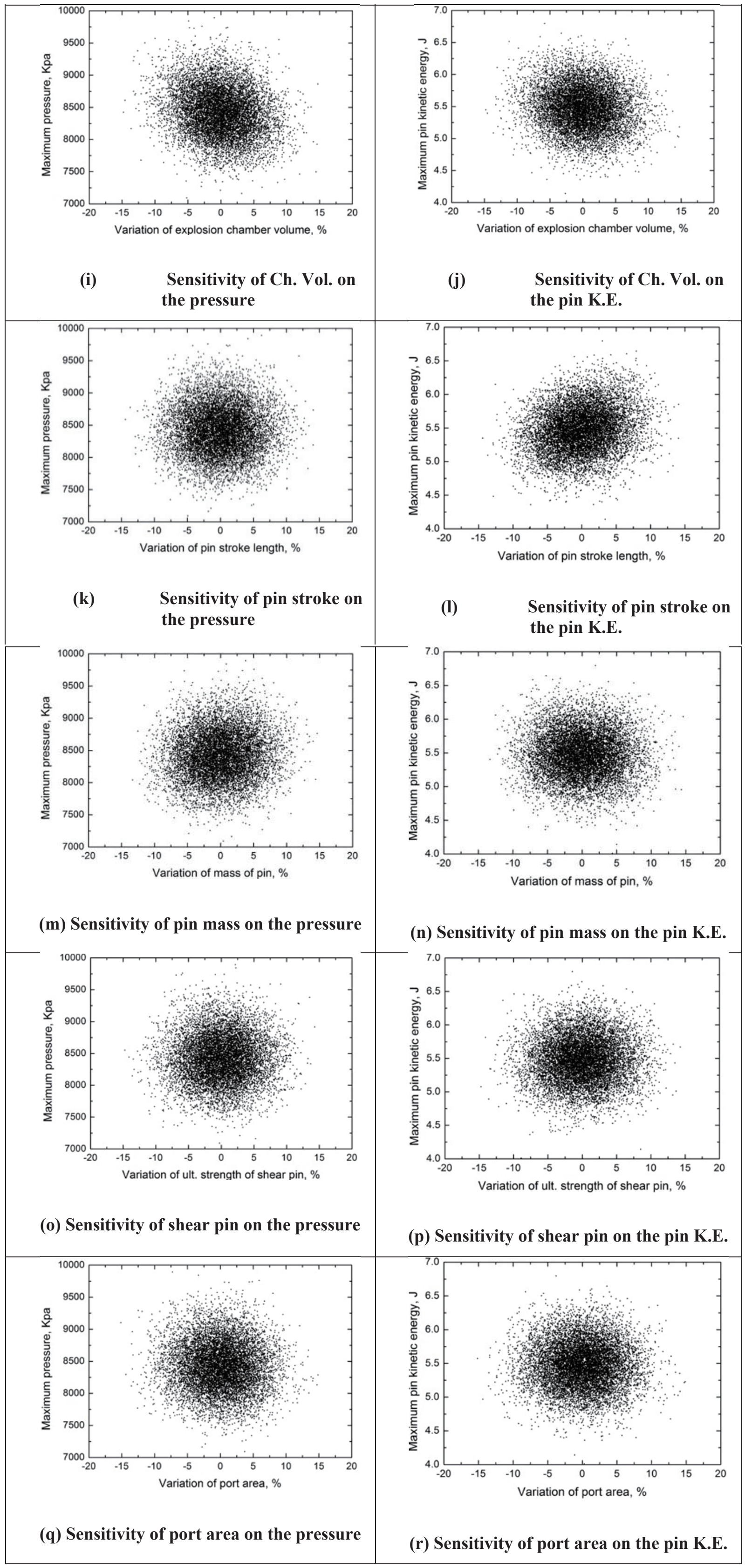

(i) Sensitivity of Ch. Vol. on the pressure

(j) Sensitivity of Ch. Vol. on the pin K.E.

(k) Sensitivity of pin stroke on the pressure

(l) Sensitivity of pin stroke on the pin K.E.

(m) Sensitivity of pin mass on the pressure

(n) Sensitivity of pin mass on the pin K.E.

(o) Sensitivity of shear pin on the pressure

(p) Sensitivity of shear pin on the pin K.E.

(q) Sensitivity of port area on the pressure

(r) Sensitivity of port area on the pin K.E.

Fig. 8. Results of the sensitivity analysis in the form of scatter plots

effective with respect to the K.E., slowed down when its mass increased. Also, the port area had a reduced effect on this reference design range.

In accordance with the above results, the port area and ultimate strength of the shear pin could be ignored during optimization. Also, relatively sensitive parameters such as the ZPP mass, pin cross-sectional area and initial pin position were treated carefully when designing a fitness function.

5.2 Performance optimization with a genetic algorithm

Pin pullers have to be robust, reliable and lightweight since they are usually designed for aerospace applications. The essential optimization goals in designing a pin puller are: (1) there must be sufficient pin kinetic energy for activation, (2) the pyrotechnic shock must be held to a minimum, (3) the device must be small and lightweight and (4) the device must use a small amount of ZPP for repeatable and uniform ignition. However, these requirements cannot be fully satisfied simultaneously. For example, a sufficient amount of ZPP is needed to achieve sufficient pin driving power for the mission, but this requirement conflicts with requirements (3) and (4). In addition, reduced weights always conflict with

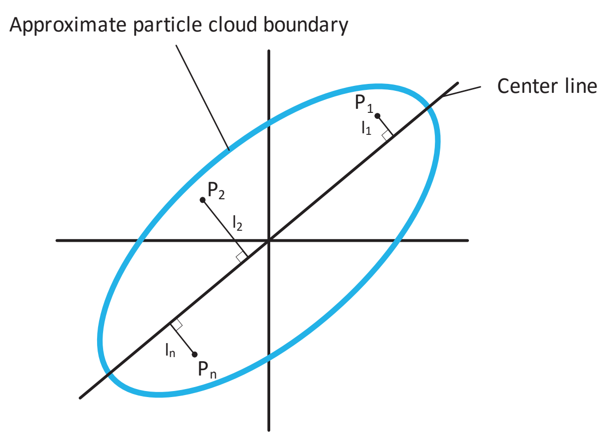

Fig. 9. Quantitative sensitivity schematics

Table 3. Normalized average distance of scattering plots

Parameters	Normalized average length of l_{avg} (or σ)	
	Maximum Pressure	Pin K.E.
ZPP mass	0.544	0.406
Pin cross section area	0.630	0.754
Initial pin position	0.797	0.871
ZPP diameter	0.828	0.942
Explosion chamber volume	0.890	0.908
Pin stroke length	0.946	0.858
Mass of a pin	0.961	0.9772
Ult. strength of shear pin	0.962	0.985
Port area	1	1

performance; this is a well-known problem in conventional engineering. In this case, appropriate trade-offs should be sought. As mentioned, pin pullers benefit from a simple mechanism, but the complex coupled design parameters makes it difficult to achieve optimal designs. Here we need a proper tool that is appropriate for multi-objective optimization.

A genetic algorithm (GA) is an optimization tool inspired by natural selection [17]. Compared to other optimization methods, a genetic algorithm is an ideal method to search out a wide range of unknown areas from the initial point (reference design). GAs determine good optimum points with proper fitness functions. Initially, the GA generates a random initial population with various individual characteristics. The information for one individual is written in a chromosome that consists of a binary number string. The fitness function, which represents complicated performance in a scalar number, is used at the next step to evaluate the fitness of each unit. After the sequence, it selects superior parents for reproduction. In the reproduction process both cross-over and mutation occur. Cross-over combines chromosomes of parents for offspring, while mutation switches one number in a string with a low probability. Mutation plays an important role when breaking the bounds of the parent's chromosome. One parental pair creates two offspring for the next generation. The performance of new generations is also evaluated by a fitness function and iterations are repeated until the population converges to an optimal solution. Applied methods and parameters for GAs are presented in Table 4. Basic GA codes are modified from the work of Carroll [18].

Design parameters for an optimal design were selected based on the results of the relative sensitivity analysis described in the previous section. According to Table 3, six parameters – the ZPP mass, pin cross-sectional area, initial pin position, ZPP diameter, explosion chamber volume and pin mass – were chosen for the GA. Note that pin stroke was excluded from the optimization process because it was one of the design requirements. Table 4 shows the cross-over method and value of each parameter used in this paper. Table 5 displays lower and upper bounds for each parameter. Limits were determined through a value of reference parameter – 200% for an upper bound and 50% for a lower bound.

Pin puller design should use multi-objective optimization concerning both weight and performance. Small devices have advantages in weight and volume, but they also tend to have difficulties in obtaining sufficient performance. An optimized trade-off design can be achieved through an appropriate fitness function. In this case, it contains the case weight, ZPP mass, operation time and designated pin kinetic energy. The objects are concerned with the weighted sum fitness function [19] presented by

$$Fitness = w_1 \frac{1}{m_{zpp}} + w_2 \frac{1}{m_{case}} + w_3 \frac{1}{t_{operation}} + w_4 e^{\frac{(KE_{pin}-6)^2}{2}} + w_5 \frac{1}{F_{ps}} \quad (28)$$

Larger ZPP amounts might lead to a higher probability of experiencing non-uniform ignition characteristics. Thus, the minimum ZPP amount is desirable. m_{case} is the total mass of the case calculated by multiplying the total surface area and minimum wall thickness that could endure the current inner pressure. This term compromises the weight and pressure since a small chamber with the same amount of ZPP induces high internal pressure. $T_{operation}$ is the operational time of the pin and is defined by the time necessary to reach maximum pin kinetic energy. The next exponential term is in the form of a normal distribution function. It denotes that the pin kinetic energy should satisfy the designed value, which is set to be 6 J in this paper. Finally, the last term drives the device to have a minimum pyrotechnic shock force. This fitness function is able to balance the optimized design between weight and performance, including short operation times, while maintaining the required pin kinetic energy. The weight coefficient, w_n, has a uniform value of 0.2 because the weight function is used to find a Pareto optimal, which is outside of the focus for this work.

Table 6 displays the parameter values of the reference and optimized designs. Both designs have a similar maximum pin kinetic energy of 6 J. Fig. 10 represents the pressure curves of the reference and optimized designs. The peak pressure is almost halved because the ZPP mass decreases about 9.0 %, the ZPP diameter increases 9.4 % and the chamber volume significantly increases (multiples of the pin cross-sectional area and the initial pin position). This induces a low chamber pressure and a long burning time. Even though the inner pressure significantly decreases, the time to peak pressure reduces because a 57 % increased pin area receives a higher pressure force, thus generating faster pin velocities, as displayed in Fig. 12. From Fig. 11, however, it is clear that the pin kinetic energy maintains its original value although all of the other parameters change due to the fourth term in Equation (27). Fig. 13 shows slightly lower forces than the reference design. The increased pin cross-sectional area and decreased chamber pressure compensate each other so as to enable the device to remain in its original position.

Overall, device shape becomes thicker because the pin diameter changes from 1.71 cm to 2.14 cm. The overall volume increases, but the weight decreases because the decreased maximum chamber pressure requires a thinner wall thickness. The increased pin cross-sectional area induces a large volume, but it produces sufficient pressure

Table 4. Subroutine method and settings for the GA

Parameters	Method	Value
Number of design parameters	-	5
Cross-over	Uniform cross-over	-
Cross-over probability	-	0.6
Mutation probability	-	0.033
Population	-	50
Iteration	-	100

Table 5. Upper and lower bounds of variables used in GA optimization

Parameters	Lower bound	Upper bound
ZPP mass (mg)	16.7	66.8
ZPP diameter (um)	24	96
Initial pin position (cm)	0.10145	0.40582
Pin cross section area (cm2)	1.1483	4.5932
Explosion cham. vol. (cm3)	0.106	0.424
Pin mass (g)	16	64

Table 6. Reference and optimized parameter values

Parameters	Reference	Optimal	Difference (%)
ZPP mass (mg)	33.4	30.38	-9.0
ZPP diameter (um)	48	52.50	9.4
Initial pin position (cm)	0.203	0.239	17.73
Pin cross section area (cm2)	2.2966	3.6123	57.29
Explosion cham. vol. (cm3)	0.212	0.192	-9.43
Pin mass (g)	32	17.52	-45.3

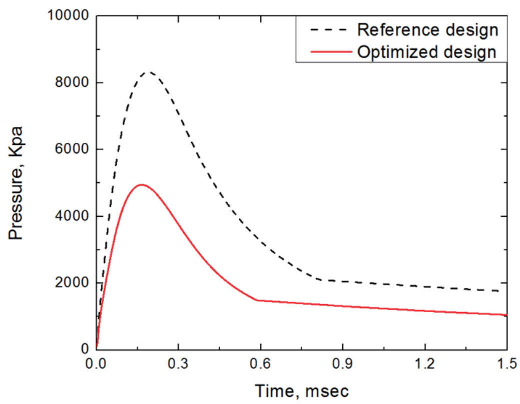

Fig. 10. Pressure of reference and optimized pin puller chambers

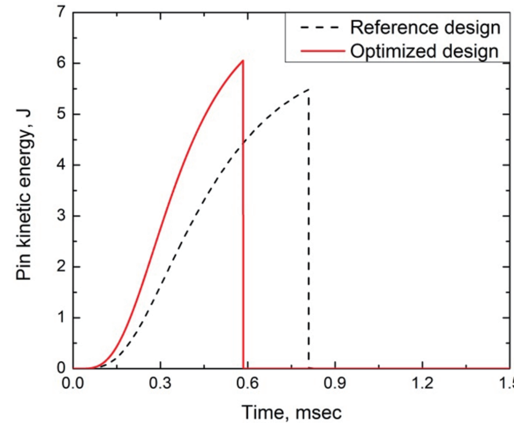

Fig. 11. Pin kinetic energy of reference and optimized pin pullers

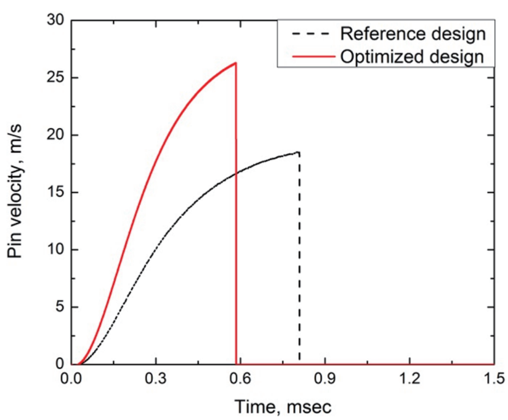

Fig. 12. Pin velocity of reference and optimized pin pullers

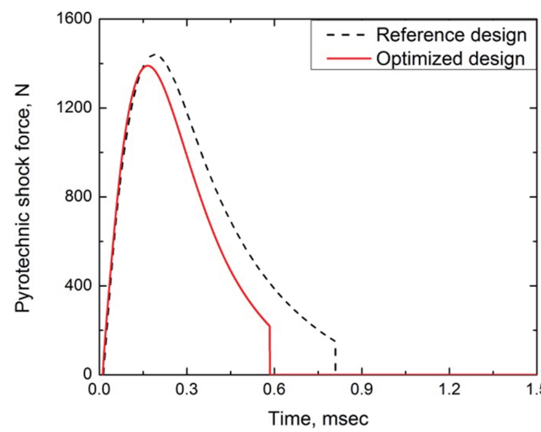

Fig. 13. Pyrotechnical shock forces of reference and optimized pin pullers

for a pushing force at low pressure. Also, the enlarged pin cross-sectional area causes a reduction in ZPP mass. This has advantages in terms of the uniform ignition of the ZPP charges. Also, the intensity of the shock wave caused by a ZPP explosion should be minimized.

6. Conclusion

A parametric study on design parameters has been conducted to observe the influence on and sensitivity to performance. Design optimization using a genetic algorithm for a pin puller has been performed based on the performance analysis technique and sensitivity analysis. The mathematical model was formulated under the assumption of an unsteady state with the uniformity of properties in each chamber. Model validation was performed by comparing the experimentally measured expansion chamber pressure with the pin displacement data. The peak pressure along with the different ZPP loading masses (33.4 and 42.9 mg) were predicted with sufficient accuracy.

Two different sensitivity analysis methods were adopted to determine the important design parameters for GA optimization. In total, nine parameters were analyzed – the ZPP mass, pin cross-sectional area, initial pin position, ZPP diameter, explosion chamber volume, pin stroke length, driving pin mass, ultimate shear pin strength and cross-sectional area of the port. The results from the OAT method presented detailed effects regarding the parameter variation to the output results and the scatter plot method implied relative sensitivity. The most sensitive parameter to the output results was the ZPP mass. However, the influence of the port area was negligible because of the relatively low chamber pressure in the reference design of this paper.

GA optimization was conducted with the ZPP mass and diameter variables, initial pin position, pin cross-sectional area, explosion chamber volume and pin mass, which were chosen through the sensitivity analysis. The fitness function was established concerning the minimum values of ZPP mass, case weight, operational time, pyrotechnic shock and targeted pin kinetic energy. The maximum peak pressure largely decreased in the optimal design because of the decreased ZPP loading mass. However, the pin kinetic energy remained constant. This was due to a widened pin cross-sectional area satisfying the sufficient pressure force at a low chamber pressure condition. Overall, the optimized design and performance changes were acceptable.

Acknowledgement

This work was supported by the Agency for Defense Development under the Precise Energy Release for the Pyrotechnic Mechanical Device program

References

[1] Brauer, O., *Handbook of Pyrotechnics*, 1st ed, Chemical Publishing Co. Inc., New York, 1974.

[2] Bement L. J. and Schimmel M. L., "A Manual for Pyrotechnic Design Development and Qualification", *NASA Technical Memorandum 110172*, 1995.

[3] DeCroix M. E., Quintana D. L., Burnett D. J., Tafoya J. M., Tafoya J. I. and Inbody M. A., "Investigation of Actuation Dynamics in an Explosively Actuated Valve Using a Gas Gun", *41st AIAA/ASME/SAE/ASEE Joint Propulsion Conference & Exhibit*, Arizona, 2005.

[4] Gonthier K. A. and Powers J. M., "Formulations, Predictions, and Sensitivity Analysis of a Pyrotechnically Actuated Pin Puller Model", *Journal of Propulsion and Power*, Vol. 10, No. 4, 1994, pp. 501-507.

[5] Paul B. H. and Gonthier, K. A., "Analysis of Gas-Dynamic Effects in Explosively Actuated Valves", *Journal of Propulsion and Power*, Vol. 26, No. 3, 2010, pp. 479-496.

[6] Lee, S. H., "Unsteady Gas Dynamics Effects in Pyrotechnic Actuators", *Journal of Spacecraft and Rockets*, Vol. 41, No. 5, 2004, pp. 877-886.

[7] Lee, S. H., "Estimating Heat Losses in Pyrotechnic Devices", *41st AIAA/ASME/SAE/ASEE Joint Propulsion Conference & Exhibit*, Arizona, 2005.

[8] Powers, J. M. and Gonthier, K. A., "Sensitivity Analysis for a Pyrotechnically Actuated Pin Puller Model", *19th International Pyrotechnics Seminar*, New Zealand, Feb. 1994.

[9] Frey, H. C. and Patil, S. R., "Identification and Review of Sensitivity Analysis Methods", *Risk Analysis*, Vol. 22, No. 3, 2002, pp. 553-578.

[10] Chan, Y. H., Correa, C. D. and Ma, K. L., "The Generalized Sensitivity Scatterplot", *IEEE Transactions on Visualization and Computer Program*, Vol. 19, No. 10, 2013, pp. 1768-1781.

[11] Berger, B., Brammer, A. J. and Charsley, E. L., "Thermomicroscopy Studies on the Zirconium-Potassium-Perchlorate-Nitrocellulose Pyrotechnic System", *Thermochimica Acta*, Vol. 269, 1995, pp. 639-648.

[12] CEA, *Chemical Equilibrium Application*, NASA Reference Publication 1311, October 1994.

[13] John, J. and Keith T., Gas dynamics, 3rd ed, Pearson Education, New Jersey, 2006.

[14] Gonthier, K. A., Kane, T. J. and Power, J. M., "Modeling Pyrotechnic Shock in a NASA Standard Initiator Driven Pin Puller", *30th AIAA/ASME/SAE/ASEE Joint Propulsion Conference*, Indianapolis, 1994.

[15] Jang, S., Lee, H. and Oh, J., "Performance Modeling of a Pyrotechnically Actuated Pin Puller", *International Journal of Aeronautical and Space Sciences*, Vol. 15, No.1, 2014, pp. 102-111.

[16] Woods, S. S., Keddy, C. P., Julien, H. and Saulsberry, R., "Estimation of Temperature and Other Properties in Pyrotechnic Reactions Using Pressure Measurements and Application of Thermodynamic Equilibrium Code", *44th AIAA/ASME/SAE/ASEE Joint Propulsion Conference*, Hartford, 2008.

[17] Davis, L., *Handbook of Genetic Algorithm*, 3rd ed, Van Nostrand Reinhold, New York, 1991, Chap 1.

[18] Carroll, D. L., "Chemical Laser Modeling with Genetic Algorithm", *AIAA Journal*, Vol. 34, No. 2, 1996, pp. 338-346.

[19] Cvetkovic, D. and Parmee, I. C., "Genetic Algorithm-based Multi-objective Optimization and Conceptual Engineering Design", *IEEE Congress on Evolutionary Computation*, Washington D.C., 1999.